NUKLEONIKA 2025;70(3):59–77
doi: 10.2478/nuka-2025-0007

REVIEW PAPER

sciendo

A review of emerging trends in experimental, simulation, and theoretical methods for dose calculation in radiation processing

Okky A. Firmansyah,
Budhy Kurniawan,
Bimo Saputro,
Marta Walo,
Urszula Gryczka,
Nunung Nuraeni

Abstract. Dosimetry serves as the backbone of ionizing radiation treatment in radiation processing, ensuring precision and accuracy in transferring the absorbed dose for medical sterilization and phytosanitary applications. Over the years, methods for calculating and measuring the absorbed dose have significantly advanced. Although experimental dosimetry remains indispensable, simulation techniques – such as Monte Carlo (MC) methods – have gained prominence by providing deeper insights into the physical processes of radiation interactions. Additionally, theoretical methods continue to provide accurate dose calculations, contributing to the field's progress. This study examines recent advancements in dose calculation techniques for radiation processing, highlighting individual methods – experimental, simulation-based, and theoretical – as well as their combinations to achieve accurate and reproducible dose measurements. It also addresses the challenges associated with each radiation processing method and discusses future prospects for improving the dosimetry of radiation processing techniques.

Keywords: Gamma irradiator • Monte Carlo • Radiation processing

O. A. Firmansyah
Department of Physics, Faculty of Mathematics and Natural Science, University of Indonesia
Depok Banten 16424, Indonesia
and Research Center for Safety, Metrology, and Nuclear Quality Technology, Research Organization for Nuclear Energy, National Research and Innovation Agency
South Tangerang, Banten 15314, Indonesia

B. Kurniawan✉
Department of Physics, Faculty of Mathematics and Natural Science, University of Indonesia
Depok Banten 16424, Indonesia
E-mail: budhy.kurniawan@sci.ui.ac.id

B. Saputro, N. Nuraeni
Research Center for Safety, Metrology, and Nuclear Quality Technology, Research Organization for Nuclear Energy, National Research and Innovation Agency
South Tangerang, Banten 15314, Indonesia

M. Walo, U. Gryczka
Institute of Nuclear and Chemistry Technology
Dorodna St. 16, 03-195 Warsaw, Poland

Received: 10 March 2025
Accepted: 7 May 2025

Introduction

Ionizing radiation has emerged as a pivotal technology for food processing and medical device sterilization [1–3]. High doses (>1 kGy) are essential for effective medical device sterilization, while precise control is necessary to maintain food quality, particularly in processes like pest disinfestation, which require significantly lower doses (<1 kGy) [4, 5]. Moreover, the Asia-Pacific region has shown a notable trend in adopting irradiation as a phytosanitary measure, particularly for tropical fruits that are distinct from the Asian continent [6]. These applications highlight the effectiveness of irradiation as a versatile and reliable option. Consequently, strict adherence to international guidelines for dose measurement systems is imperative to ensure consistent irradiation quality across radiation processing facilities.

Accurate dosimetry is a critical component of successful irradiation processes, ensuring the delivery of an appropriate radiation dose for the intended application [7]. To achieve this, three primary methods are commonly used in the radiation processing field: experimental measurement, simulation, and theoretical calculation. Experimental dosimetry involves direct measurements using dosimeters placed within or around the irradiated material, providing

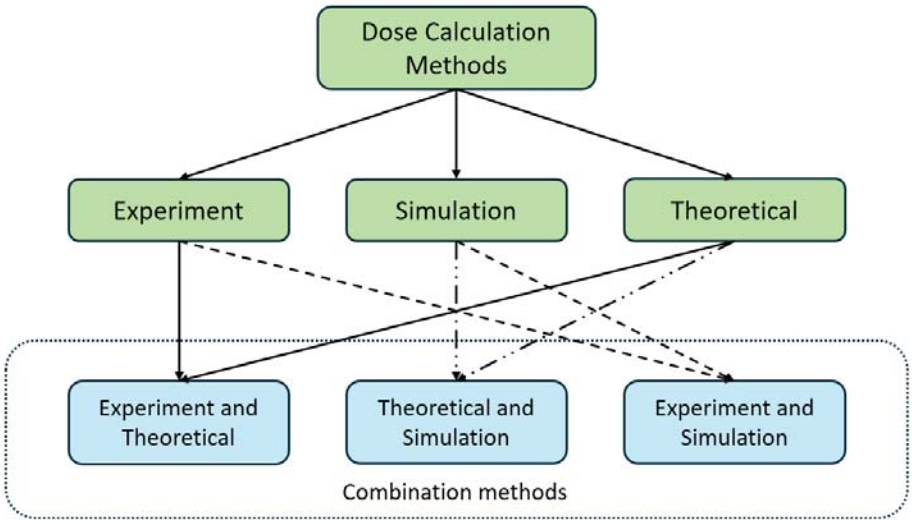

Fig. 1. Schematic diagram of dose calculation methods.

precise dose values under actual conditions [7]. Simulation methods, often leveraging the widely used Monte Carlo (MC) code system, offer a robust means of calculating doses while providing valuable insights into the complex physical interactions between radiation and matter [8, 9]. Complementing these is the theoretical method, which applies fundamental physics and mathematical principles to estimate the absorbed doses [10].

Although experimental methods remain the backbone of dose measurement, they have certain limitations, particularly in terms of flexibility and accessibility. Challenges arise when dealing with complex geometries, such as irregularly shaped food items or fruits or large-scale objects, which require numerous dosimeters for accurate measurements [10, 11]. In such cases, MC simulations have become indispensable for predicting dose distributions, especially in scenarios where direct measurements are impractical [12, 13]. These simulations enable detailed modeling of radiation interactions with various materials, providing highly accurate predictions of the absorbed dose [9]. On the contrary, theoretical methods, while being advantageous in reducing the costs associated with experimental dosimeters, present their own challenges. Their reliance on complex mathematical formulations and the time required to complete calculations can be prohibitive for some researchers. In addition, they still need to be validated with experimental measurements due to some factors, such as the conditional environment, which can cause different results in dose measurements [10].

Using these methods together reveals how their strengths can help to solve the challenges of radiation processing. In addition to the three methods mentioned above, combining two methods enhances the validity of the research. Simulation studies require validation through experimental methods to ensure the reliability of the models [8, 14]; otherwise, the results cannot be trusted for understanding physical interactions. Similarly, theoretical methods are validated using either simulation or experimental methods to confirm the accuracy of theoretical calculations [15, 16]. Each method, whether used independently or in combination, has distinct advantages and disadvantages.

Although significant researches have been conducted on dose calculation methods, few articles have specifically addressed emerging trends in this field. This presents an ideal opportunity for a review article to consolidate and provide an updated perspective on the current status of this evolving research area. This study explores recent advancements in dose calculation techniques for radiation processing, with a particular focus on the combination of experimental, simulation-based, and theoretical methods to ensure accurate, effective, and consistent outcomes. The literature review, conducted using the Google Scholar database, employed keywords related to various absorbed dose calculation methods for radiation processing. This study examines these methods across major modalities, including gamma irradiators, electron beam systems, and X-ray facilities, while addressing the challenges inherent to each method. In addition, it considers the practical implications of dose calculations to ensure process reliability, meet regulatory standards, and foster innovation in radiation processing applications.

Absorbed dose as the quantity of interest

The absorbed dose (D) represents the amount of ionizing radiation deposited in a material, which, in the context of radiation processing, may include food products, medical devices, or material standards. In simpler terms, it quantifies the radiation energy absorbed by a material per unit mass. The international unit (SI) for the absorbed dose is Gray (Gy), where 1 Gy is equivalent to the absorption of 1 joule (J) of energy per kilogram (kg) of material (1 J/kg) [17]. Understanding the absorbed dose is crucial for applications in radiation processing, where precise measurement and traceability are essential.

To ensure accuracy and reliability in dose measurements, the absorbed dose has traditionally been measured using calorimeter systems [18]. The water

calorimeter serves as the primary standard for disseminating the absorbed water dose, which is the key quantity of interest. This instrument is essential for various applications in medical physics and radiation processing [19, 20]. Despite the inherent complexity of calorimetry, this method is highly reliable and can achieve low uncertainties, typically <1.0% [18].

Although primary standards like the water calorimeter ensure high precision, routine dosimeters such as polystyrene-based ones are preferred for their practicality in industrial settings. In radiation processing, a polystyrene-based calorimeter is commonly used as a routine dosimeter rather than as a primary standard [21, 22]. Unlike the water calorimeter, which relies on high-precision supporting instruments, the polystyrene dosimeter typically features a simpler construction. A key difference between the two lies in measurement uncertainty: the water calorimeter, as a primary standard, typically achieves a relative combined standard uncertainty of <1.0% [18], whereas the polystyrene calorimeter exhibits a higher uncertainty, around 3.6% [23, 24], both reported with a coverage factor of $k = 2$.

To bridge the gap between high-precision primary standards and practical routine dosimetry, the absorbed dose quantity is transferred to secondary standard dosimeters [19, 25]. In radiation processing, alanine dosimeters are widely utilized as secondary standards due to their robustness and well-established measurement characteristics, including temperature correction, signal fading, and electron spin resonance (ESR) techniques [26]. Furthermore, the water equivalency of alanine material enhances its suitability for precise dose measurements, particularly in the context of absorbed dose realization methods. This calibration chain ensures consistency and accuracy, enabling reliable dose measurements across diverse radiation processing applications. Subsequently, the traceability of these measurements can be extended to routine dosimetry systems, which are employed in daily operational dose monitoring.

Absorbed dose calculation methods

Experimental method

Experimental methods form the backbone of dose measurements because they reflect the actual conditions of the measurement process. However, achieving accurate results requires a solid understanding of both fundamental dosimetry principles and measurement techniques. Equally important is maintaining traceability for both the dosimeter and reader, as this directly impacts the quality of the measurements and, consequently, the quality of the irradiated product [7]. When a dosimetry system is well-established, it can provide both high precision and accuracy in dose measurements, ensuring reliable outcomes and maintaining the integrity of the irradiation process.

Building on the foundation of established dosimetry systems, recent studies have focused on addressing challenges in dose measurement by highlighting two key areas: development of dosimeter and measurement techniques. While several commercially available dosimeters are widely used for dose measurement, they often face limitations, particularly in specific applications such as food irradiation, where the required dose range can be restrictive [7]. These challenges have spurred the exploration of novel measurement techniques aimed at optimizing the performance of commercial dosimeters and enabling their more effective application across a range as stated by the manufacturer.

Review

Development of the dosimeter. Motivated by the demand for alternative dosimeters in the radiation processing field, several studies have concentrated on developing dosimeters that can measure high-dose ranges. As shown in Table 1, most of these dosimeters are classified as passive dosimeters, each with a specific dose range. Passive dosimeters require a post-irradiation period to allow the material to stabilize and for the radiation-induced interactions within the material to fully develop [27]. The stabilization phase is important for ensuring accurate and reliable dose measurements for proper functioning.

The development of high-dose dosimetry has seen significant advancements using diverse materials and methodologies, reflecting a focus on optimizing performance across various radiation types and energy levels. As shown in Table 1, these dosimeters are based on unique material properties, such as thermoluminescent [14, 28], optical [29], and spectroscopic characteristics, to achieve precision in dose measurement. The integration of advanced materials, including phosphors [30, 31], optical fibers [29], and polymer films [32], has enabled accurate assessments even at microscale thicknesses and in complex geometries. In addition to advancements in dosimeter materials, classical techniques such as UV–Vis spectrophotometry [32, 33], luminescence decay measurements [30], and electron paramagnetic resonance (EPR) spectroscopy [34] have become integral tools, offering high sensitivity and adaptability across dose ranges extending to kilogray.

Schuster *et al*. [30] introduced a novel approach for relative dose measurement on object surfaces. Recognizing the critical need for accurate surface dose determination in irradiated objects, this method employs a phosphor-based dosimeter that is directly sprayed onto the object's surface. This approach allows the dosimeter to conform precisely to the object's shape, enabling accurate and reliable dose measurements. Luminescence readings were performed using a custom-designed in-house 3D reader. The proposed technique was benchmarked against the B3 film dosimeter and further validated through simulation studies. Results showed that a micro-size dosimeter was in good agreement with both the existing dosimeters and the simulation data. This method is particularly effective for low-dose electron beams (80–200 keV) and for measuring doses within the first 3–4 μm of material thickness [31].

Table 1. List of articles focusing on the development of the dosimeter

Dosimeter	Beam	Shape	Dose range	Reader	Uncertainty	Reference
TLD-doped silica fibers	Gamma	Fiber with a cylinder shape with a diameter of 8.5 μm for core and 125 μm for cladding	Up to 20 Gy	Harshaw 3500 TL reader	N/A	[14, 28]
Radiochromic film containing poly(hexa-2,4-diynylene adipate)	Gamma	1 cm × 1 cm size sheets; thickness 0.037 ± 0.004 mm	0.5–65 kGy	UV–Vis's spectrophotometer (the measurement wavelength is 520 nm)	5.5% (2σ)	[33]
Inorganic phosphor particles, NaYF4:Yb3+ and Er3+	Low-energy (80/140/200 keV) electron beam	Liquid spray (1.6 μm thickness)	5–30 kGy	The luminescence decay time of the phosphor was recorded via the photocurrent of a silicon photodiode (Osram SFH2200) equipped with a 980 nm band-pass filter (BrightLine 980/10)	15% (2σ)	[30, 31]
Silica optical fiber scintillators	Electron beam (1 MeV)	Fiber with a cylinder shape with a diameter of 600 μm for core and 630 μm for cladding	10–70 kGy	Hamamatsu C10082Ca spectrometer (luminescence spectra wavelengths from 200 nm to 800 nm)	N/A	[29]
PVA films with different concentrations of MTB dye	Gamma	Liquid stored in 3 ml glass ampoules	2.5–20 kGy (for film) and 0.1–1.2 kGy (for solution)	UV–Vis spectrophotometry (Shimadzu, Japan); the wavelength ranges from 350 nm to 700 nm	N/A	[32]
High-density polyethylene (A4009)	Gamma; electron beam (2.5 MeV)	30 mm × 20 mm × 28 μm	25–1000 kGy	NICOLET Magna IR-750 spectrometer	N/A	[35]
Fructose	Gamma	0.5 g of clip plastic	0.05–30 kGy	MiniScope MS5000 EPR spectrometer	N/A	[34]
High-density polyethylene	Gamma; electron beam (2.5 MeV)	30 mm × 4 mm × 28 μm	5–193 kGy (for gamma); 5–300 kGy (for electron)	Bruker ER 200D spectrometer	N/A	[36]

Table 2. A list of articles focusing on the development of measurement methods

Dosimeter type	Key results	Method	Beam	Year	Reference
EBT3 Gafchromic film	Extending the sensitivity of the EBT3 film to high doses up to 100 Gy while ensuring low-dose uncertainty	An optical setup involving a broadband light source, a fiber optic probe working in reflection configuration, and a spectrometer was used to detect changes in the spectral response of several EBT3 films	250 kV X-rays and 1 MeV electron beam	2020	[37]
Alanine	Determine a scaling factor to convert a dose determination using alanine based on Co-60 calibration to give the dose delivered in a high-energy electron beam	This study combines the alanine dose results of experimental and simulation studies	≥6 MeV electron beam	2020	[41]
PMMA	Introducing a new dosimetry method called Z-scan to optimize the PMMA dosimeter	The Z-scan system was used to measure the non-linear optical properties of the PMMA dosimeter. A He-Cd laser beam (442 nm, 150 mW) was used for this system	Gamma	2021	[40]
Alanine	A correction factor that can be used for alanine to measure the kilovoltage is X-rays	Combined experimental and MC simulation codes for measuring the dose at several X-rays beam quality	20–180 keV X-rays	2022	[38]
Alanine	A model to calculate the relative efficiency of alanine pellets in low-energy X-ray beams	A microdosimetric one-hit detector model was used to characterize the detector's intrinsic efficiency. Geant4-DNA MC simulations estimated microdosimetric distributions, with literature data providing the free model parameters	Low (40–170 kV) and medium X-rays (100–300 kV)	2022	[45]
B3 film	Understanding the effect of heating the B3 film dosimeter on performance	DSC was used to analyze the thermal properties of B3 radiochromic dosimetry films. The glass transition temperature (T_g) and decomposition behavior of irradiated and non-irradiated films were studied	Low-energy electron beam (200 kV)	2022	[42]
Gafchromic MD-V3 and HD-V2 films	Understanding the effect of temperature on dose measurement during irradiation	Gafchromic MD-V3 and HD-V2 were irradiated at various temperatures, and their optical density	Gamma	2022	[43]

These advances represent a positive progress in the development of high-dose dosimeters, offering improved accuracy and compatibility with both gamma- and electron-beam radiation. They enhance the ability to measure radiation doses with fine detail, even on complex surfaces [30, 31]. This progress not only strengthens the capabilities of dosimetry and paves the way for the development of novel dosimeters but also expands applications in precise radiation measurements.

Optimization of the measurement methods. The optimization of dosimetry depends on the development of accurate and reliable measurement methods, as illustrated by the studies summarized in Table 2. Recent research has focused on optimizing commercially available dosimeters to extend dose ranges [37] and measurement fields [38, 39]. This includes the introduction of novel methods for reading dosimeter responses [40] and the implementation of new correction factors [41].

Innovative approaches, such as the Z-scan system for PMMA dosimeters [40] and optical fiber setups for Gafchromic films [37], emphasize the need for precise quantification of radiation doses. These methods are particularly critical in scenarios in which environmental factors, such as temperature and beam quality, significantly affect dosimeter responses. Addition-

ally, studies involving B3 films [42] and Gafchromic MD-V3 and HD-V2 films [43] have highlighted the importance of external parameters, such as temperature, in optimizing dosimeter performance.

The alanine dosimeter has long been used as a secondary standard and transfer dosimeter in radiation processing [19, 25]. Conventionally, alanine with the EPR system has been used to measure absorbed doses in electron beam and gamma radiation [7]. However, recent studies have demonstrated that alanine can also be effectively applied to X-ray dosimetry by incorporating a correction factor to account for its response to low- and medium-energy X-rays [38, 44, 45]. These advancements highlight the development of new methods that not only enhance the versatility and reliability of alanine dosimeters but also address challenges in dose determination accuracy across different radiation energy levels. As the use of X-ray machines emerges in industrial radiation processing, this research will support the dosimetry of X-rays [46].

On the contrary, Malcolm McEwen made a significant contribution by introducing a scaling factor to convert the dose measured with alanine dosimeters irradiated at Co-60 to doses applicable for electron beam qualities [41]. This approach has been applied in medical physics for >25 years and remains a reliable method for accurate dosimetry [47]. The scaling factor is determined through a consensus approach by combining experimental and simulation methods to establish precise values. Since alanine dosimeters are typically traceable to the absorbed dose to water for Co-60 beam qualities, this scaling factor is particularly beneficial when extending their use to electron beam measurements. However, incorporating the scaling factor into the absorbed dose measurement requires careful consideration of its contribution to the overall uncertainty budget.

Challenges and outlooks

One of the challenges associated with experimental approaches, often determined by user experience, is selecting the appropriate dosimeter for irradiation processing [7]. Key considerations include the dose range, thickness, and post-irradiation stability time. For applications such as food irradiation and medical device sterilization, the dosimeter thickness does not always accurately represent the surfaces being measured [30, 31]. Additionally, positioning the dosimeter within the object can be challenging, often leading to low-precision dose measurements.

Another significant issue is the post-irradiation stabilization time required to obtain reliable readings. Given the demand for rapid dose measurements in the field, alanine dosimeters are not commonly used as routine options owing to their lengthy stabilization time and high operational costs. This highlights the need for dosimeters with shorter post-irradiation stabilization times as well as improved methods for precise positioning during measurements. These highlights represent promising research and innovation.

For many years, polystyrene calorimeters have been a standard tool in the radiation processing field [21]. However, recent advancements indicate a growing interest in developing active dosimeters for use in ultra-high-dose applications in medical physics [48, 49]. This technology can be adapted for the radiation processing field, as it shares similarities with high-dose rate requirements. Such adaptation would require modifications to account for positioning challenges and dose variations. These developments present a valuable opportunity for future calorimetry research.

Simulation method

The main reason for employing simulation methods in radiation processing is to accurately predict the dose distribution and to deepen the understanding of radiation interactions to improve irradiation techniques. Radiation processing facilities are often large-scale and handle complex-shaped objects, as they are typically used for mass-irradiation activities [11, 50]. This scale and complexity pose challenges in maintaining the quality of dosimetry. Unique issues arise within the dosimetry system, such as the need for precise measurements, numerous dosimeters, and careful calibration to ensure consistent and reliable results. Simulation methods address these challenges effectively by providing accurate and detailed dose calculations, thereby enabling better control and optimization of the irradiation process and reducing operational costs.

Simulation methods rely on computer programming to obtain the desired physical quantities. Two main methods are commonly used in radiation fields: the point-kernel method and the MC method [9]. Both methods use random number generation to model the stochastic nature of radiation. The point-kernel method, which is widely applied in nuclear medicine [51, 52], is advantageous for calculating point doses. However, its limitations in modeling complex objects and its focus on point dose calculations make it unsuitable for radiation processing. In contrast, the MC method is preferred for radiation processing because of its flexibility. It allows for detailed modeling of both irradiation facilities and the objects being irradiated, making it the optimal choice for applications requiring comprehensive and precise simulations [9].

Several MC-based software applications are commonly employed in ionizing radiation research, including PENELOPE [53], Geant4 [54], EGSnrc [55], MCPNX [53], RT-office [56], PUFFin [57], FLUKA [58], and PHITS [59]. Each of these software programs uses distinct algorithms and configurations. In a study by El-Ouardi, a comparison between MCNP6 and Geant4 revealed a compatibility result of <9.0% when compared with the Fricke dosimeter [60]. These differences in the simulation results are often attributed to variations in the algorithm design of each software, which can affect the cross-sections, physical models, number of generated pseudorandom numbers, and numerical estimates used to model the trajectories of photons and electrons through materials.

Review

Recent studies on the use of MC simulations in radiation processing have primarily focused on two areas: facility modeling and food irradiation. Table 3 lists the articles that specifically addressed MC simulations for facility modeling and food irradiation.

Facility modeling plays an important role in supporting dose mapping, a key component of operational qualification activities. As shown in Table 3, these facilities are categorized as first and second gamma irradiators, which have relatively smaller geometries than the larger fourth category [14, 25, 61, 62]. Despite their smaller size, these configurations can present challenges due to the high number of radiation sources, which can include up to 48 individual sources [61]. In contrast, fourth category irradiators involve much larger geometries, such as large totes that require detailed modeling. For example, Tran Van Hung's dose mapping study modeled 68 tote boxes, each with dimensions of 50 cm × 50 cm × 90 cm [50]. Futher classification and comparison of these facility categories can be found in the sub-section discussing the combination and simulation methods..

Particular attention must be given to the activity and measurement dates of each Co-60 radionuclide because variations in these parameters can significantly affect the dose distribution. Furthermore, not all manufacturers ensure a uniform distribution of pencil sources across all pencil slots, leading to non-uniform radiation source distribution [63]. This variability increases the complexity of achieving consistent dose distribution within the facility. To address these challenges effectively, it is crucial to thoroughly examine the facility design drawings to obtain accurate geometric details. Proper geometry is essential for creating precise models that reflect the actual configuration of the facility, ensuring reliable dose mapping and operational accuracy.

In addition to gamma irradiators, there are studies modeling machine-based sources, such as electron beam and X-ray irradiation facilities [46, 64]. However, only a few studies have focused on the detailed modeling of machine-based sources, presenting comprehensive modeling concepts in their publications [64, 65]. While other studies involving electron beams exist, they do not specifically address e-beam modeling in detail [11, 58, 66].

Accurate e-beam modeling requires careful configuration of the nominal electrical current to realistically represent the operational conditions of the facility. The e-beam and X-ray facility modeling share similar complexities with the gamma plant modeling. For instance, Eychenne obtained MC spectrum results from an X-ray facility in Aerial, France [46]. The radiation spectrum, whether from electron beams or X-rays, is a critical factor because beam quality can vary across facilities. Ideally, the spectrum produced by MC modeling should closely approximate a realistic electron or X-ray spectrum to ensure that dose calculations align with experimental results.

Another unique challenge addressed by MC approaches is estimating the dose of fruit phytosanitary irradiation. By employing MC simulations, accurate dose estimations can be achieved without generating fruit waste. This method is particularly valuable for food materials with complex shapes, such as broccoli, chicken, and fruits, where traditional methods may be less efficient or wasteful [11]. From both technical and economic perspectives, direct measuring of doses in fresh products is often not ideal for quality control in mass-production processes, although it remains a common practice for dose mapping [67].

Both facility modeling and food irradiation modeling share a common focus on physical quantities, specifically the calculation of absorbed doses, whether as dose distribution or specific doses in targeted regions. However, their areas of emphasis differ. In food irradiation, the dose distribution is primarily observed on the fruit surface, particularly when using electron beams [58, 68]. This focus aligns with the goal of phytosanitary irradiation, which targets the fruit surface where pest eggs are typically laid [69]. In contrast, for industrial facilities, the focus of dose distribution is on identifying regions with the best dose uniformity to optimize processing efficiency and product quality, thereby completing the performance qualification steps [8, 50, 70].

In MC modeling studies that do not involve experimental validation, the emphasis is often placed on understanding the physical interactions within the simulated processes. While some studies present results in absolute terms, this is usually because the MC model has already been validated in previous research. For instance, Jongsoon Kim's series of publications over the past decade (2005, 2007, 2010, 2011, 2013, 2015, 2019) includes early works with validation, allowing later studies to focus solely on simulation without revalidating the model [67, 71–76]. Conversely, some studies presented results in relative terms rather than absolute values, especially when no experimental validation was conducted.

In addition, MC studies without experimental validation often enable the rapid exploration of various parameters and configurations, which may be difficult or costly to replicate through experimental means. This flexibility makes MC modeling an invaluable tool for preliminary assessments and hypothesis testing. By adjusting variables such as geometry, source strength, and material composition, researchers can investigate potential outcomes without the need for extensive laboratory setups. A representative example is the study conducted by Moradi *et al*., which employed MC simulations to design a mini collimator for use in a Category I Gamma Cell with the goal of improving the dose uniformity ratio [61]. This work exemplifies the strength of MC methods in allowing for the modeling of various components and evaluating their effects as part of an important design analysis before fabrication. The study systematically compared multiple collimator configurations, including different shapes and materials, to identify the most effective design. As a result, the manufacturing process could be directed toward a single optimized model, improving both cost-efficiency and the accuracy of subsequent experimental measurements.

Table 3. A list of articles focusing on MC simulation studies related to radiation processing facilities and food irradiation modeling

Type	Object	Beam	MC code	Parameters	Year	Reference
Modeling of radiation processing facilities	USA, JS-7500 MDS Nordion (first category, dry storage)	Co-60, Gamma	MCNPX	Dose profile	2021	[61]
	Tunisia, C-188 MDS Nordion France (second category, dry storage)	Co-60, Gamma	MCNPX	Isodose curve	2021	[54]
	Malaysia, Gamma cell (first category, dry storage)	Co-60, Gamma	MCNPX	Dose profile	2021	[61]
Food irradiation modeling	Melon (USA)	Electron beam 1.35 MeV and 10 MeV	MCNP-5	Dose distribution, depth-dose curve	2010	[67]
	Egg (USA)	10 MeV (high-energy) and 1.35 MeV (low-energy) for electron beams, 5 MeV for X-rays, and 1.25 MeV for gamma rays	MCNP-5	Dose distribution, depth-dose curve	2011	[71]
	Pineapple (USA)	2 MeV (low-energy) and 10 MeV (high-energy) for electron beams, 1.25 MeV for gamma rays, and 5 MeV for X-rays	MCNP-5	Dose distribution, depth-dose curve	2013	[72]
	Mangosteen (USA)	Electron beam (high-energy) and 1.35 MeV (low energy); 5 MeV for X-rays; and 1.25 MeV for Co-60 gamma rays	MCNP-5	Dose distribution, depth-dose curve	2014	[77]
	Mangoes (USA)	1.25 MeV from a Co-60 source	MCNP-5	Dose distribution, depth-dose curve	2015	[73]
	Potatoes, onion (India)	2 MeV, 5 MeV, and 10 MeV electron beams	MCNPX2.6	Dose distribution, depth-dose curve	2018	[78]
	Pine (USA)	10 MeV electron beam and 1.25 MeV gamma rays	MCNP-5	Dose distribution, depth-dose curve	2019	[74]
	Egg (Japan)	80-kV electron beam	PHITS	Surface and inside dose	2023	[79]
	Apple (Iran)	Electron beam = 500 keV; X-ray = 200 kV	Geant4	Dose distribution, depth-dose curve	2023	[58]

In addition to its powerful capability to simulate radiation interactions, simulation studies must validate their findings to ensure accuracy. MC simulations offer flexibility in modeling objects and allow for the use of assumptions when specific details or specifications are unavailable. Therefore, validation through experimental data or benchmarking against established models is essential to confirm the reliability of the simulations. This process not only enhances the credibility of the findings but also ensures that the results can be effectively applied in real experiments, such as optimizing radiation processes or improving facility designs.

Challenges and outlooks

The challenges in the MC approach include (i) accurately modeling objects, particularly in assigning their mass density, (ii) the limited ability of MC simulations to account for dynamic rather than static objects, and (iii) the complexity of the program preparation. These challenges represent key limitations of the MC approach, despite its notable advantages in understanding physical processes and estimating the absorbed dose. Nonetheless, MC estimation results are generally acceptable compared with experimental data if they fall within the expanded uncertainty range of the dosimeter.

Fruit modeling was conducted using two methods: model based on DICOM images obtained from computer tomography (CT) scans and CAD model [58, 67]. Using DICOM images and converting them into MC code provided a more accurate way to mimic the fruit's geometry. However, this approach does not account for the true mass density distribution within the fruit. Real fruits often have varying mass densities, even within a single layer of flesh. The conventional approach involves simplifying the fruit into two distinct regions with different mass densities: the flesh and seeds. These two regions were assigned separate mass densities, a method commonly used in MC-based fruit studies. Although this method is effective, the accuracy of fruit modeling can be further enhanced by assigning the true density distribution for each region of the fruit.

The latest development of the PHITS MC code introduced a feature to convert DICOM images into MC code, automatically defining mass density based on the gray values of CT numbers (Hounsfield units [HU]) [80]. However, this feature was primarily designed for human tissue and not for fruits. Therefore, the conversion of a fruit's CT numbers to its mass density still requires validation to ensure accuracy. Nevertheless, accurately measuring fruit density remains a significant challenge.

Another significant challenge associated with the MC approach is its limitation in simulating dynamic objects, whether in the context of fruit studies or irradiation facilities. In the case of MC simulations for fruit, this issue was addressed by Jongsoon Kim [68] and Kataoka [79], who introduced object rotation to mimic dynamic movement. Their method involved manually rotating the object to various angles and averaging the absorbed dose across the rotations. This approach demonstrated good agreement with expectations and provided valuable insights into uniform irradiation across the object's surface.

For irradiation facilities, a key challenge lies in modeling the transit dose in Type I irradiators, such as Gamma-Cell or Gamma-chamber systems. The transit dose refers to the radiation dose absorbed by the sample during its movement from the initial position to the irradiation position [8]. While the transit dose is generally measured in the order of Gray (Gy), it becomes critical when the target dose is also in the Gy range. However, it is less problematic when the target dose is kilogray (kGy). Accurate modeling of transit doses in these systems remains a complex task. Mannai *et al*. [81] addressed this challenge by calculating the transit dose at three distinct time points along the sample chamber's transfer path, summing the dose from all sampling points. More recently, El-Ouardi [82] employed a semi-analytical approach combined with MC simulations to calculate the transit dose. Their method, inspired by Mannai's work, focused on shorter time intervals (4–35 s) to improve the accuracy of the simulations [82].

The challenge of addressing dynamic motion in MC simulations has been overcome using updated MC codes, specifically 4D Monte Carlo (4D MC) codes. These codes incorporate time as a fourth dimension in addition to conventional 3D geometry (X, Y, Z) axes [83, 84]. The primary application of 4D MC has been in medical physics, particularly for dose reconstruction and verification in scenarios involving dynamic organ motion [85]. By integrating time into dose calculations, 4D MC significantly improved accuracy compared with conventional static models. However, these advanced features increase computational demands, requiring high-performance computing systems to achieve reliable results with low uncertainties.

Looking ahead, 4D MC simulations offer a promising solution to address the challenges posed by dynamic motion in radiation processing facilities. One example of an MC code used for this purpose is EGSnrc/4DdefDOSXYZnrc, an extension of the EGSnrc system that incorporates time-dependent geometry and deformation capabilities [83, 85]. The application of 4D MC methods may extend beyond first-category gamma irradiators to include fourth-category systems and electron beam facilities, where objects are continuously transported via conveyors during irradiation. This dynamic modeling approach enhances both the accuracy and efficiency of dose calculations in time-dependent irradiation scenarios.

The third challenge associated with the MC approach is the complexity involved in program preparation. Developing an accurate MC model and obtaining the desired output, such as dose distribution, can take hours or even days. This process is impractical for radiation processing facilities because of the limited time and computational resources. However, a recent advancement in MC code development, released in 2024, introduced a tool called PUFFin (Penelope User-Friendly Fast Interface), which represents a breakthrough in simplifying the MC process [57]. This innovative tool allows users

Table 4. Studies related to theoretical methods for processing radiation

Year	Calculation method	Physical parameter	Object	Author	Reference
2006	Multipole moment	Flux	Co-60 pencils	Loussaief A.	[86]
2007	Multipole moment	Dose	Co-60 pencils	Loussaief A.	[87]
2016	Haar Wavelet Numerical method	Flux	Co-60 pencils	Belkadhi K.	[89]
2017	Haar Wavelet Numerical method	Flux	Irradiated products with different densities	Belkadhi K.	[15]
2017	Multipole moment	Flux	Co-60 pencils	Rezaeian P.	[88]
2020	TOPSIS	Dose	Irradiated product (box)	Singh M.	[90]
2023	Voronoi diagram	Dose	Irradiated product (box)	Singh M.	[10]

to input a 2D image and run simulations with ease. Its intuitive graphical user interface (GUI) offers a "plug-and-play" experience, making the process more accessible and efficient. With these advantages, it is hoped that the MC code will become a reliable daily tool for accurately estimating absorbed doses in mass-radiation processing.

Theoretical method

Review

Flux and dose calculations. Finally, the theoretical method is another significant method for dose calculation in radiation processing. Several studies (Table 4) have explored this method, including the implementation of the multipole moment method, which has been employed by various researchers to calculate photon flux in irradiators [86–88]. The multipole moment method is a robust analytical technique that facilitates the calculation of charge or mass distributions in systems such as electromagnetic fields. The reduction of complex three-dimensional problems into manageable analytical forms enables precise modeling of photon flux, particularly in irradiation facilities where uniformity and dose control are critical. Therefore, this method is highly effective for determining both the flux and dose, and it can contribute to improve design and optimization of irradiation systems.

To better understand how the multipole moment method achieves these results, the process can be divided into three key steps. First, the source distribution is defined by specifying the positions and activities of each element in the gamma source array, such as pencil sources or Gamma cell units. Second, the moments are calculated by integrating the source distribution over space, typically using Cartesian coordinates (x, y, z), to account for the strength of the source relative to the point at which the dose is estimated. Finally, the coefficients of the multipole moments are determined through direct analytical integration or by fitting simulation data, such as those generated by MCNP simulations. Advanced techniques, like the Levenberg–Marquardt algorithm, are often used to fine-tune these coefficients, ensuring precise and reliable results [88].

Optimization of the dose mapping. Using a different method, Menghraj Singh, in two notable studies, focused on optimizing dosimeter placement in pallet boxes to ensure consistent and accurate dose delivery in radiation processing [10, 90]. In his first study [90], he integrated the analytical hierarchy process (AHP) model with the technique for order preference by similarity to ideal solution (TOPSIS) model. This combination enables a systematic evaluation of multiple placement strategies by considering various criteria, such as dose uniformity, cost, and operational efficiency. In his second study, he employed the Voronoi diagram model, a geometric method that uses spatial partitioning to determine the optimal distribution of dosimeters within a pallet. By identifying regions with potential dose variations, this method improves coverage and reduces uncertainties in dose delivery.

Furthermore, Singh extended the Voronoi diagram-based method to model product boxes and optimize dosimeter positioning on vertical planes. By incorporating Delaunay triangulation and Voronoi vertices, the study demonstrated improved dose uniformity with a lower overdose ratio compared with traditional methods [10]. Notably, the Voronoi method achieved a dose uniformity ratio of 1.06, outperforming the conventional ratio of 1.07. This advancement highlights the potential to enhance commissioning dosimetry processes and overall irradiation efficiency. The visibility and applicability of this method in actual radiation processing underscore its promise as a tool for improving dose accuracy and operational efficiency in various industrial applications.

In addition to its performance benefits, the Voronoi diagram-based method offers significant resource optimization. Singh demonstrated that this method reduced the number of dosimeters required for dose mapping to 56 units compared with the 126 units needed in conventional methods to cover all dose points [10]. This reduction not only streamlines the process but also enhances the efficiency of dose mapping, making it a highly effective solution for improving quality assurance in radiation processing.

Challenges and outlooks

Theoretical methods, such as those based on the multipole moment method, offer powerful tools for dose and flux calculations in radiation processing [87, 88]. However, their practical implementation faces significant challenges. One of the key issues is the validation of theoretical results against experi-

mental data, as accurately reproducing the actual irradiation conditions in a theoretical framework can be complex. Additionally, these methods often require extensive computational resources, particularly when dealing with high-resolution models or large irradiation systems. Integrating diverse optimization approaches, such as the AHP and TOPSIS, with physical modeling frameworks add another layer of complexity.

Another significant challenge in theoretical methods is the variability in the source activity, geometry, and material properties, which can lead to discrepancies between the theoretical predictions and experimental outcomes. Theoretical methods typically rely on the assumption of ideal conditions to model objects; however, in practice, these ideal conditions are often unattainable. For example, the material properties of an object, such as its density, may vary because of its manufacturing processes, introducing uncertainties into the model. Such variations underscore the need for robust validation to ensure that theoretical models accurately reflect the complexities of actual conditions.

Despite these challenges, theoretical radiation processing methods are promising. Advances in computational algorithms, such as adaptive mesh refinement and machine learning, are expected to streamline the modeling process, making it faster and more accessible. Enhanced validation protocols, including benchmarking against MC simulations and experimental data, will further strengthen the confidence in these models. Resource optimization, as demonstrated by Singh's Voronoi diagram approach, highlights the potential to reduce dosimeter usage and enhance dose mapping efficiency.

Combinations of the methods

Experimental and theoretical results

Unfortunately, there are only a few examples of studies that combine experimental and theoretical approaches in dose calculations for radiation processing. In such cases, the experimental approach is often used as a reference for validating the results of theoretical methods. As discussed in the section on theoretical approaches, Rezaian used Amber dosimeters for dose measurement and obtained good agreement between the measurements and theoretical calculations [88]. Similarly, Singh used ceric-cerous dosimeters in his study for dose mapping measurements optimized with the Voronoi diagram algorithm [10].

These findings underscore the potential benefits of integrating experimental and theoretical methods to enhance the accuracy of dose calculations. However, this integration faces challenges, particularly in terms of understanding the fundamental physics of the models. In addition, theoretical approaches often rely on assumptions that may deviate from the actual measurement conditions. Although theoretical methods may be well-suited for research, they are less practical for large-scale irradiation processing because of time constraints.

Theoretical and simulation

A series of studies focused on optimizing aluminum plates to reduce electron beam doses demonstrated the effective combination of theoretical and simulation approaches [16, 91–94]. Specifically, the Geant4 MC code was employed for dose calculations to provide a detailed understanding of the underlying physics of the experiments, as outlined in their publications. These studies considered not only the relative depth dose but also the spectrum of the electron beam after passing through the aluminum foil [94, 95].

However, one key issue is the complexity associated with accurately modeling the physical interactions of electron beams with materials, which require computational resources and expertise. Additionally, the assumptions and simplifications made in the simulations, such as the idealized material properties and beam conditions, may not fully represent the actual material, potentially leading to discrepancies between the theoretical predictions and experimental results. These limitations highlight the need for careful validation of models against experimental data to ensure reliability and applicability in practical settings.

Experimental and simulation

In Tables 5 and 6, studies on irradiation facilities are predominantly based on MC simulation results that have been validated through experimental measurements using dosimeters. In contrast, Table 3 presents only the MC modeling results without any experimental validation. Validating MC simulations is a critical step in ensuring the accuracy of outcomes, which is typically performed by comparing simulation data with experimental dose measurements obtained using dosimeters. As shown in Table 5, the relative differences between the simulation and experimental results ranged from 1.0% to 12.0%. Not every measurement point in an MC simulation requires validation; instead, representative points can be selected for validation.

A solid understanding of dosimetry concepts – such as dosimetry quantities, positioning, build-up regions, dosimeter functionality, and external factors affecting measurements – is essential for radiation dose measurements. This understanding directly affects the agreement between the MC simulation and experimental validation. In MC simulations, the dosimeter model must accurately reflect the experimental conditions, including factors such as dosimeter density, placement, and the presence or absence of build-up material. For example, Majer *et al*. modeled a partial hip prosthesis and validated the simulation using an ethanol-chlorobenzene (ECB) dosimeter [8]. The position of the dosimeter in the simulation was adjusted to match its position in the experimental setup, resulting in good agreement between the experimental and simulation results, with a relative difference of $<5.0\%$.

A similar approach was used for validating the MC modeling in fruit irradiation by comparing

Table 5. A list of MC modeling for irradiation facilities

Country/irradiator type	Year	Irradiator categories	Beam	Software MC	Parameters	Experiments	Agreement MC/EXP	Reference
Iran, IR-136 irradiator	2002	IV. Wet storage	Co-60, Gamma	MCNP	Isodose curve, absorbed dose, and dose rate	PMMA, Fricke, ECB, potassium dichromate dosimeter	2.0–6.0%	[96]
	2002	IV. Wet storage	Co-60, Gamma	MCNP	Absorbed dose	PMMA, Fricke, ECB, potassium dichromate dosimeter	2.0–6.0%	[97]
Iran, Gamma Cell	1993	I. Dry storage	Co-60, Gamma	EGS4	Dose rate, flux	Fricke	<5.0%	[98]
	2017	I. Dry storage	Co-60, Gamma	MCNP	Flux distribution	PMMA	Good agreement	[88]
USA, JS-7500 MDS Nordion	2003	IV wet storage	Co-60, Gamma	ITS/ACCEPT MC Code	Absorbed dose	FWT-60	2.0–5.0%	[99]
Portugal, UTR GAMA-Pi	2000	II. Dry storage	Co-60, Gamma	MCNP 4B2	Dose rate	Amber perspex and cericaceous dosimeters	Max. deviation = 1.08%	[100]
	2000	II. Dry storage	Co-60, Gamma	MCNP	Flux, Air Kerma Rate	Ion chamber	Max. deviation 12%, avg. MC/EXP = 0.968	[101]
	2007	II. Dry storage	Co-60, Gamma	MCNPX	Dose rate	Fricke	Avg. MC/EXP = 0.947 and 1.102, respectively	[102]
	2008	II. Dry storage	Co-60, Gamma	MCNPX, PENELOPE	Isodose curve and dose rate	Fricke	Deviation 2.0–3.0%	[53]
	2010	II. Dry storage	Co-60, Gamma	MCNPX	Dose rate (per second)	Ion chamber and PMMA dosimeter	Good agreement	[103]
Tunisia, C-188 MDS Nord	2005	II. Dry storage	Co-60, Gamma	Geant4	Dose rate and isodose curve	Red Perspex, Gammachrome PMMA	Avg. deviation of 6.0% (>6.0% for 6 data points)	[104]
	2005	II. Dry storage	Co-60, Gamma	Geant4	Isodose curve and dose uniformity	Red Perspex, Gammachrome PMMA	Avg. deviation of 5.0%	[105]
	2007	II. Dry storage	Co-60, Gamma	Geant4	Dose, dose rate, transit dose	Red Perspex, Gammachrome PMMA	Good agreement	[81]
	2017	II. Dry storage	Co-60, Gamma	Geant4	Absorbed dose, dose rate, dose uniformity, and isodose curve	PMMA	<3.0%	[106]
South Korea, C-188 MDS Nord	2008	II. Dry storage	Co-60, Gamma	MCNPX	Dose rate	Ion chamber and MOSFET dosimeter	Max. deviation = 3.0%	[107]
South Korea, EB Tech	2023	N/A	2.5 MeV electron beam	MCNP 6.2	Relative dose	CTA film dosimeter	Good agreement	[108]

Table 5. Continued

Country/irradiator type	Year	Irradiator categories	Beam	Software MC	Parameters	Experiments	Agreement MC/EXP	Reference
UK, JS-7500 MDS Nordion	2009	Wet storage	Co-60, Gamma	EGSnrc	Dose rate	Ion chamber and alanine	Max. deviation 2.0% (IC) and 4.0% (alanine)	[55]
Vietnam/SVST-Co60 B VINAGAMA	2010	IV. Wet storage	Co-60, Gamma	MCNP-4C	Absorbed dose, dose rate, and dose uniformity	ECB	Max. deviation = 6.0%	[50]
Vietnam	2021	N/A	UERL-10-15S2 linear accelerator	MCNP4c	Relative depth dose	B3 WINdose	<6.0%	[64]
Syria	2013	Wet storage	Co-60, Gamma	MCNP-4C	Dose rate	ECB	4.0–7.0%	[109]
Bangladesh	2018	II. Dry storage	Co-60, Gamma	MCNPX 2.7	Absorbed dose and dose rate	Fricke and cerebral	Max. deviation 12%	[110]
Brazil, GB-127 MDS Nordion	2017	II. Dry storage	Co-60, Gamma	MCNPX	Dose rate and isodose curve	Fricke	Max. deviation = 8.03%	[111]
	2017	II. Dry storage	Co-60, Gamma	MCNPX 2.6	Absorbed dose, dose rate, isodose curve	Fricke	Max. deviation = 9.0%	[112]
	2019	II. Dry storage	Co-60, Gamma	MCNPX 2.9	Absorbed dose, dose rate, isodose curve	Fricke	Max. deviation 21%	[113]
Malaysia, Gamma cell	2017	I. Dry storage	Co-60, Gamma	MCNP	Dose rate and spectrum	TLD (silica fiber dosimeter)	Max. deviation 6.7%	[14]
Croatia	2019	I. Dry storage	Co-60, Gamma	Geant4	Dose rate, transit dose	Ion chamber	5.0–8.0% (Avg. 6.0%)	[70]
	2024	I. Dry storage	Co-60, Gamma	PHITS	Dose rate	Ion chamber: ECB	Max. deviation = 5.0%	[8]
Morocco, Co-60	2020	II. Dry storage	Co-60, Gamma	MCNPX	Dose rate and isodose curve	Alanine	Max. deviation 7.3%	[114]
	2020	II. Dry storage	Co-60, Gamma	MCNPX	Dose rate and isodose curve	Alanine	Max. deviation = 9.0%	[115]
	2020	II. Dry storage	Co-60, Gamma	MCNPX	Dose rate	Fricke	Max. deviation = 9.0%	[60]
	2021	II. Dry storage	Co-60, Gamma	MCNPX	Dose rate	Alanine	Max. deviation = 9.0%	[62]
	2023	II. Dry storage	Co-60, Gamma	Geant4	Transit dose	Fricke	Max. deviation = 9.0%	[82]
France	2022	N/A	X-ray	MCNPX 2.7, RayXpert	Dose rate, isodose curve, dose-uniformity ratio, spectrum	Alanine	2.4% and 4.1%	[46]

Table 6. A list of MC modeling for another irradiated object

Year	Object	Software MC	Parameters	Experiments	Agreement MC/EXP	Reference
2021, 2023	Egg	PHITS	Dose and dose distribution	RCD, FWT60-180, Far West Technology	Good agreement	[79, 116]
2021	Cables	MCNP 6.2	Energy deposition (MeV/g)	CTA film dosimeter	Good agreement	[66]
2024	Aluminum, ethafoam, wood, polystyrene	PUFFin	Depth-dose distribution	CTA, B3-layer film; FWT-60, full-length	Good agreement	[57]

the simulation results with the experimental dose measurements. In a study, Jongsoon Kim compared the simulation results with dose measurements taken on an apple phantom using an in-house dosimeter phantom and radiochromic film [68]. A good agreement was observed between the MC simulation and experimental measurements, with a difference of not more than 5.0%. This close match validated both the simulation results and the dosimetry phantom development, confirming the accuracy of the measurements.

The choice of the dosimeter significantly affects the experimental results and measurement methods. Beyond the dose range, other performance characteristics of the dosimeter must also be carefully considered. For example, validating dose measurements for fruits presents unique challenges because of the high water content in fruits, which can influence dosimeter performance. If the dosimeter is not waterproof, the measurements may not be reliable. Additionally, the selection and placement of dosimeters on the fruit have a significant impact on ensuring accurate dose measurement results. Small-volume dosimeters are typically preferred for point-dose measurements, as they provide more precise measurement at specific locations. For assessing dose distribution, film dosimeters are often favored because of their good spatial resolution and detailed representation of the absorbed dose across the surface.

Conclusion

Dosimetry is fundamental to effective irradiation treatments, primarily focusing on experimental methods, such as measuring absorbed doses in real objects using dosimeters. However, optimizing the irradiation process requires a deeper understanding of the underlying physical interactions. In this context, MC simulations and theoretical methods offer reliable dosimetry calculations. Each method has its advantages and limitations, particularly in terms of dose range, dosimeter thickness, calibration, and environmental conditions, all of which influence the precision of the absorbed dose quantification.

To obtain valid results, combining different methods provides a robust approach while enabling cross-validation. These combinations can take several forms: (i) experimental and theoretical, (ii) theoretical and simulation, and (iii) experimental and simulation. Combining experimental and theoretical methods, for instance, faces challenges, particularly in terms of understanding the fundamental physics underlying the models. Moreover, theoretical approaches often rely on assumptions that may not fully align with actual measurement conditions. Additionally, the time required for dose calculations using theoretical methods can be a limitation, especially for radiation processing services that demand rapid results.

Integrating the MC simulation results with the experimental validation provides the most robust solution for dosimetry studies. This approach combines the strengths of both methods: MC simulations provide detailed insights into radiation interactions and dose distributions, while experimental validation ensures the accuracy and traceability of measurements. Together, these methods significantly improve the precision of radiation dose measurements, making them particularly valuable for large-scale industrial applications. Moreover, with the variety of MC codes available, users can select the most suitable and efficient option to streamline performance qualification processes, enabling timely validation before irradiation.

Despite advancements in dosimetry methods for radiation processing, limitations persist, underscoring the need for continued innovation and development in measurement techniques. Addressing these gaps effectively requires further exploration and refinement of existing methods. By addressing these challenges, researchers can enhance dose calculation methods and unlock new opportunities in dosimetry, leading to more efficient and precise radiation processing technologies.

Acknowledgment. The authors express sincere gratitude to Dr. Budhy Kurniawan and Dr. Nunung Nuraeni for their invaluable time and insightful discussions. Special thanks are extended to Mr. Bimo Saputro for his extensive contributions in discussions on various aspects of the radiation processing field. The authors are also deeply thankful to Urszula Gryczka and Marta Walo for sharing their expertise and offering constructive suggestions that greatly enhanced the quality of this paper.

Funding. No funding was provided to support this manuscript.

Author contribution. Okky Agassy Firmansyah: Writing, original draft, formal analysis, and conceptualization. Budhy Kurniawan and Nunung Nuraeni: Writing–review and editing, visualization, and supervision. Bimo Saputro, Marta Walo, and Urszula Gryczka: Supervisory and editing.

Generative AI and AI-assisted technologies in the writing process. During the preparation of this work, the author(s) used ChatGPT-4 and TRINKA AI to refine grammar and address systematic writing errors, as the author(s) are non-native English speakers. After using this tool/service, the author(s) reviewed and edited the content as necessary and took full responsibility for the final content of the published article.

Conflict of interest. The authors declare that there are no conflicts of interest related to the research, authorship, or publication of this manuscript.

ORCID

O. A. Firmansyah https://orcid.org/0000-0002-0068-5703
U. Gryczka https:/orcid.org/0000-0003-2221-4176
B. Kurniawan https://orcid.org/0000-0002-9203-7438
N. Nuraeni https://orcid.org/0000-0003-0148-3334
B. Saputro https://orcid.org/0000-0003-2888-5130
M. Walo https://orcid.org/0000-0002-5115-6334

References

1. Colletti, A. C., Denoya, G. I., Vaudagna, S. R., & Polenta, G. A. (2024). Novel applications of gamma irradiation on fruit processing. *Curr. Food Sci. Technol. Rep*., *2*(1), 55–64. https://doi.org/10.1007/s43555-024-00016-w.
2. Bisht, B., Bhatnagar, P., Gururani, P., Kumar, V., Tomar, M. S., Sinhmar, R., Rathi, N., & Kumar, S. (2021). Food irradiation: Effect of ionizing and non-ionizing radiations on preservation of fruits and vegetables–a review. *Trends Food Sci. Technol*., *114*, 372–385. https://doi.org/10.1016/j.tifs.2021.06.002.
3. Chaudhary, S., Kumar, S., Kumar, V., Singh, B., & Dhiman, A. (2024). Irradiation: A tool for the sustainability of fruit and vegetable supply chain–advancements and future trends. *Radiat. Phys. Chem*., *217*, 111511. https://doi.org/10.1016/j.radphyschem.2024.111511.
4. Li, D., Bisel, T. T., Cooley, S. K., Ni, Y., Murphy, M. K., Spencer, M. P., Hasan, Md K., Fifield, L. S., Pharr, M., Staack, D., Huang, M., Pillai, S. D., Nichols, L., Parker, R., & Gustin, E. (2025). Gamma, electron beam and X-ray irradiation effects on polymers in an advanced bone cement mixer device. *Radiat. Phys. Chem*., *226*, 112188. https://doi.org/10.1016/j.radphyschem.2024.112188.
5. Akter, H., Cunningham, N., Rempoulakis, P., & Bluml, M. (2023). An overview of phytosanitary irradiation requirements for Australian pests of quarantine concern. *Agriculture*, *13*(4), 1–15. https://doi.org/10.3390/agriculture13040771.
6. Ihsanullah, I., & Rashid, A. (2017). Current activities in food irradiation as a sanitary and phytosanitary treatment in the Asia and the Pacific Region and a comparison with advanced countries. *Food Control*, *72*, 345–359. https://doi.org/10.1016/j.foodcont.2016.03.011.
7. Kuntz, F., & Strasser, A. (2016). The specifics of dosimetry for food irradiation applications. *Radiat. Phys. Chem*., *129*, 46–49.
8. Majer, M., Pasariček, L., & Knežević, Ž. (2024). Dose mapping of the ^{60}Co gamma irradiation facility and a real irradiated product – Measurements and Monte Carlo simulation. *Radiat. Phys. Chem*., *214*, 111280.
9. Saputro, B., Saputro, A. H., & Nuraeni, N. (2024). A Monte Carlo approach for predictive tools in gamma irradiator: a review. *J. Radioanal. Nucl. Chem*., 0123456789. https://doi.org/10.1007/s10967-024-09871-2.
10. Singh, M., Datta, D., & Gupta, A. (2023). Modelling and optimization of dosimeters in the product box for commissioning dosimetry at gamma irradiator using Voronoi Diagram algorithm. *Radiat. Phys. Chem*., 210, 111011. https://doi.org/10.1016/j.radphyschem.2023.111011.
11. Rivadeneira, R., Kim, J., Huang, Y., Castell-Perez, M. E., & Moreira, R. (2007). A 3-D dosimeter for complex-shaped foods using electron-beam irradiation. *Am. Soc. Agric. Biol. Eng*., *50*(5), 1751–1758.
12. Andreo, P. (1991). Monte Carlo techniques in medical radiation physics. *Phys. Med. Biol*., *36*(7), 861–920.
13. Andreo, P. (2018). Monte Carlo simulations in radiotherapy dosimetry. *Radiat. Oncol*., *13*(1), 1–15. https://doi.org/10.1186/s13014-018-1065-3.
14. Moradi, F., Khandaker, M. U., Mahdiraji, G. A., Ung, N. M., & Bradley, D. A. (2017). Dose mapping inside a gamma irradiator measured with doped silica fibre dosimetry and Monte Carlo simulation. *Radiat. Phys. Chem*., *140*, 107–111. https://doi.org/10.1016/j.radphyschem.2017.01.032.
15. Belkadhi, K., Elhamdi, K., Bhar, M., & Manai, K. (2017). Dose calculation using Haar wavelets with buildup correction. *Appl. Radiat. Isot*., *127*, 186–194. https://doi.org/10.1016/j.apradiso.2017.06.011.
16. Zolotov, S. A., Bliznyuk, U. A., Studenikin, F. R., Borshchegovskaya, P. Y., & Krusanov, G. A. (2023). Combination of aluminum plates of different thicknesses to increase the homogeneity of radiation treatment by accelerated electrons. *Phys. Part. Nucl. Lett*., *20*(4), 954–958.
17. Knoll, G. F. (2010). *Radiation detection and measurement* (4th ed.). John Wiley & Sons.
18. Renaud, J., Palmans, H., Sarfehnia, A., & Seuntjens, J. (2020). Absorbed dose calorimetry. *Phys. Med. Biol*., *65*(5), 05TR02. DOI: 10.1088/1361-6560/ab4f29.
19. McEwen, M. R., Sharpe, P. H. G., Pazos, I. M., Miller, A., Pawlak, E., Ninlaphruk, S., Zhang, Y., & Kessler, C. (2022). Supplementary comparison CCRI(I)-S3 of standards for absorbed dose to water in ^{60}Co gamma radiation at radiation processing dose levels. *Metrologia*, *59*(1A), 1–18. DOI: 10.1088/0026-1394/59/1A/06012.
20. Muir, B. R., Cojocaru, C. D., McEwen, M. R., & Ross, C. K. (2017). Electron beam water calorimetry measurements to obtain beam quality conversion factors. *Med. Phys*., *44*(10), 5433–5444.

21. Miller, A. (1995). Polystyrene calorimeter for electron beam dose measurements. *Radiat. Phys. Chem*., *46*(4/6), 1243–1246.
22. Miller, A., & Kovacs, A. (1990). Application of calorimeters for routine and reference dosimetry at 4–10 MeV industrial electron accelerators. *Radiat. Phys. Chem*., *35*, 774–778.
23. Miller, A., Kovacs, A., & Kuntz, F. (2002). Development of polystyrene calorimeter for application at electron energies down to 1.5 MeV. *Radiat. Phys. Chem*., *63*, 739–744.
24. ISO/ASTM International. (2013). ISO/ASTM 51631: Practice for use of calorimetric dosimetry systems for electron beam dose measurements and routine dosimetry system calibration.
25. International Atomic Energy Agency. (2002). *Dosimetry for food irradiation*. Vienna: IAEA. (TRS no. 409).
26. Secerov, B., Radenkovic, M., & Dramicanin, M. (2016). Uncertainty and routine use of aerial L-alanine – electron spin resonance dosimetry system. *Radiat. Meas*., *89*, 63–67. https://doi.org/10.1016/j.radmeas.2016.03.003.
27. Yang, Z., Vrielinck, H., Jacobsohn, L. G., Smet, P. F., & Poelman, D. (2024). Passive dosimeters for radiation dosimetry: Materials, mechanisms, and applications. *Adv. Funct. Mater*., *34*(41), 2406186. https://doi.org/10.1002/adfm.202406186.
28. Mahdiraji, G. A., Ghomeishi, M., Dermosesian, E., Hashim, S., Ung, N. M., Adikan, F. R. M., & Bradley, D. A. (2015). Optical fiber based dosimeter sensor: Beyond TLD-100 limits. *Sens. Actuators A-Phys*., *222*, 48–57. https://doi.org/10.1016/j.sna.2014.11.017.
29. Oresegun, A., Basaif, A., Tarif, Z. H., Abdul-Rashid, H. A., Hashim, S. A., & Bradley, D. A. (2021). Radioluminescence of silica optical fibre scintillators for real-time industrial radiation dosimetry. *Radiat. Phys. Chem*., *188*, 109684. https://doi.org/10.1016/j.radphyschem.2021.109684.
30. Schuster, C., Kuntz, F., Strasser, A., Härtling, T., Dornich, K., & Richter, D. (2021). 3D relative dose measurement with a μm thin dosimetric layer. *Radiat. Phys. Chem*., *180*, 109238.
31. Schuster, C., Kuntz, F., Cloetta, D., Zeller, M., Katzmann, J., Strasser, A., Härtling, T., & Lavalle, M. (2022). Depth dose curve and surface dose measurement with a μm thin dosimetric layer. *Radiat. Phys. Chem*., *193*, 109881. https://doi.org/10.1016/j.radphyschem.2021.109881.
32. Rabaeh, K. A., Aljammal, S. A., Eyadeh, M. M., & Abumurad, K. M. (2021). Methyl thymol blue solution and film dosimeter for high dose measurements. *Results Phys*., *23*, 103980. https://doi.org/10.1016/j.rinp.2021.103980.
33. Soliman, Y. S., Abdel-Fattah, A. A., & Alkhuraiji, T. S. (2018). Radiochromic film containing poly(hexa-2,4-diynylene adipate) as a radiation dosimeter. *Appl. Radiat. Isot*., *141*, 80–87. https://doi.org/10.1016/j.apradiso.2018.08.016.
34. Rachmanto, A., Putri, M. A. E., Yunus, M. Y., Yunus, A. L., Fitriana, R., & Rahmawati, R. (2024). ESR spectroscopic analysis of fructose as a dosimeter for gamma radiation. *Nucl. Instrum. Methods Phys. Res. Sect. B-Beam Interact. Mater. Atoms*, *557*, 165551. https://doi.org/10.1016/j.nimb.2024.165551.
35. Al-Ghamdi, H., Farah, K., Almuqrin, A., & Hosni, F. (2022). FTIR study of gamma and electron irradiated high-density polyethylene for high dose measurements. *Nucl. Eng. Technol*., *54*(1), 255–261. https://doi.org/10.1016/j.net.2021.07.023.
36. Khouqeer, G. A., Farah, K., Toumi, S., & Hosni, F. (2025). Electron paramagnetic resonance characterization of gamma and electron irradiated high-density polyethylene: Possible use as a high-dose dosimeter. *Nucl. Eng. Technol*., 103419. https://doi.org/10.1016/j.net.2024.103419.
37. Vaiano, P., Consales, M., Casolaro, P., Campajola, L., Fienga, F., Di Capua, F., Breglio, G., Buontempo, S., Cutolo, A., & Cusano, A. (2019). A novel method for EBT3 Gafchromic films read-out at high dose levels. *Phys. Med*., *61*, 77–84. https://doi.org/10.1016/j.ejmp.2019.04.013.
38. Nasreddine, A., Kuntz, F., & El Bitar, Z. (2021). Absorbed dose to water determination for kilo-voltage X-rays using alanine/EPR dosimetry systems. *Radiat. Phys. Chem*., *180*, 108938. https://doi.org/10.1016/j.radphyschem.2020.108938.
39. Hjørringgaard, J. G., Ankjærgaard, C., Miller, A., & Andersen, C. E. (2023). Kilovoltage X-ray beam quality effect on the relative response of alanine pellet dosemeters. *Radiat. Prot. Dosim*., *199*(14), 1605–1610. https://doi.org/10.1093/rpd/ncad008.
40. Beigzadeh, A. M., & Vaziri, M. R. R. (2021). Z-scan dosimetry of gamma-irradiated PMMA. *Nucl. Instrum. Methods Phys. Res. Sect. A-Accel. Spectrom. Dect. Assoc. Equ.*, *991*, 165022. https://doi.org/10.1016/j.nima.2021.165022.
41. McEwen, M., Miller, A., Pazos, I., & Sharpe, P. (2020). Determination of a consensus scaling factor to convert a Co-60-based alanine dose reading to yield the dose delivered in a high energy electron beam. *Radiat. Phys. Chem*., *171*, 108673. https://doi.org/10.1016/j.radphyschem.2019.108673.
42. Skowyra, M. M., Ankjærgaard, C., Yu, L., Lindvold, L. R., Skov, A. L., & Miller, A. (2022). Glass transition temperature of Risø B3 radiochromic film dosimeter and its importance on the post-irradiation heating procedure. *Radiat. Phys. Chem*., *194*, 109982. https://doi.org/10.1016/j.radphyschem.2022.109982.
43. Yamada, H., & Parker, A. (2022). Gafchromic TM MD-V3 and HD-V2 film response depends little on temperature at time of exposure. *Radiat. Phys. Chem*., *196*, 1–7.
44. Hjørringgaard, J. G., Ankjærgaard, C., Bailey, M., & Miller, A. (2020). Alanine pellet dosimeter efficiency in a 40 kV x-ray beam relative to cobalt-60. *Radiat. Meas*., *136*, 106374. https://doi.org/10.1016/j.radmeas.2020.106374.
45. Hjørringgaard, J. G., Ankjærgaard, C., & Andersen, C. E. (2022). The microdosimetric one-hit detector model for calculating the relative efficiency of the alanine pellet dosimeter in low energy X-ray beams. *Radiat. Meas*., *150*, 106659. https://doi.org/10.1016/j.radmeas.2021.106659.
46. Eychenne, L., Vander Stappen, F., Kuntz, F., Stichelbaut, F., Dossat, C., Robin-Chabanne, S., & Chatry, N. (2022). High energy X-ray fruit irradiation qualification with Monte Carlo code. *Radiat. Phys. Chem*., *195*, 110075. https://doi.org/10.1016/j.radphyschem.2022.110075.

47. Andreo, P., Burns, D. T., Kapsch, R. P., McEwen, M., Vatnitsky, S., Andersen, C. E., Ballester, F., Borbinha, J., Delaunay, F., Francescon, P., Hanlon, M. D., Mirzakhanian, L., Muir, B., Ojala, J., Oliver, C. P., Pimpinella, M., Pinto, M., de Prez, L. A., Seuntjens, J., Sommier, J., Teles, P., Tikkanen, J., Vijande, J., & Zink, K. (2020). Determination of consensus kQ values for megavoltage photon beams for the update of IAEA TRS-398. *Phys. Med. Biol.*, *65*(9), 095011. https://doi.org/10.1088/1361-6560/ab807b.
48. Bourgouin, A., Schüller, A., Hackel, T., & Kranzer, R. (2020). Calorimeter for real-time dosimetry of pulsed ultra-high dose rate electron beams. *Front. Phys.*, *8*, 567340. https://doi.org/10.3389/fphy.2020.567340.
49. Subiel, A., & Romano, F. (2023). Recent developments in absolute dosimetry for FLASH radiotherapy. *Br. J. Radiol.*, *96*(1148), 20220560. https://doi.org/10.1259/bjr.20220560.
50. Van Hung, T., & Khac An, T. (2010). Dose mapping using MCNP code and experiment for SVST-Co-60/B irradiator in Vietnam. *Appl. Radiat. Isot.*, *68*(6), 1104–1107. https://doi.org/10.1016/j.apradiso.2010.01.023.
51. Graves, S. A., Flynn, R. T., & Hyer, D. E. (2019). Dose point kernels for 2,174 radionuclides. *Med. Phys.*, *46*(11), 5284–5293. https://doi.org/10.1002/mp.13789.
52. Papadimitroulas, P., Loudos, G., Nikiforidis, G. C., & Kagadis, G. C. (2012). A dose point kernel database using GATE Monte Carlo simulation toolkit for nuclear medicine applications: Comparison with other Monte Carlo codes. *Med. Phys.*, *39*(8), 5238–5247. https://doi.org/10.1118/1.4737096.
53. Belchior, A., Botelho, M. L., Peralta, L., & Vaz, P. (2008). Dose mapping of a ^{60}Co irradiation facility using PENELOPE and MCNPX and its validation by chemical dosimetry. *Appl. Radiat. Isot.*, *66*(4), 435–440. https://doi.org/10.1016/j.apradiso.2007.11.017.
54. El-Ouardi, Y., Aknouch, A., Dadouch, A., Mouhib, M., & Benmessaoud, M. (2021). Monte Carlo simulation as a predictive tool to program a reloading operation of a gamma irradiator. *Mosc. Univ. Phys. Bull.*, *76*(6), 482–487. https://doi.org/10.3103/S0027134921060047.
55. Bailey, M., Sephton, J. P., & Sharpe, P. H. G. (2009). Monte Carlo modelling and real-time dosemeter measurements of dose rate distribution at a ^{60}Co industrial irradiation plant. *Radiat. Phys. Chem.*, *78*(7/8), 453–456. https://doi.org/10.1016/j.radphyschem.2009.03.024.
56. Lazurik, V. T., Lazurik, V. M., Popov, G., Rogov, Y., & Zimek, Z. (2011). *Information system and software for quality control of radiation processing*. Warsaw: International Atomic Energy Agency; Institute of Nuclear Chemistry and Technology.
57. Schwarz, R., Salvat, F., Sunderland, D., Azuma, M., Boutros, C., Pillai, S., Kuntz, F., Nasreddine, A., Pagh, J., Wootan, D., & Murphy, M. K. (2024). PUFFIn – A user friendly fast interface for calculating and visualizing the dose distribution in materials. *Radiat. Phys. Chem.*, *222*, 111774. https://doi.org/10.1016/j.radphyschem.2024.111774.
58. Rafiepour, P., Sina, S., & Javad Mortazavi, S. M. (2023). A multiscale Monte Carlo simulation of irradiating a typical-size apple by low-energy X-rays and electron beams. *Radiat. Phys. Chem.*, *212*, 111016. https://doi.org/10.1016/j.radphyschem.2023.111016.
59. Iwamoto, Y., Sato, T., Hashimoto, S., Ogawa, T., Furuta, T., Abe, S. I., Kai, T., Matsuda, N., Hosoyamada, R., & Niita, K. (2017). Benchmark study of the recent version of the PHITS code. *J. Nucl. Sci. Technol.*, *54*(5), 617–635. https://doi.org/10.1080/00223131.2017.1297742.
60. El-Ouardi, Y., Dadouch, A., Aknouch, A., Mouhib, M., Maghnouj, A., & Didi, A. (2020). Comparative study between Geant4, MCNP6 and experimental results against gamma radiation comes from a cobalt-60 source. *Mosc. Univ. Phys. Bull.*, *75*(5), 507–511. https://doi.org/10.3103/S0027134920050033.
61. Moradi, F., Khandaker, M. U., Abdul Sani, S. F., Uguru, E. H., Sulieman, A., & Bradley, D. A. (2021). Feasibility study of a minibeam collimator design for a ^{60}Co gamma irradiator. *Radiat. Phys. Chem.*, *178*, 109026. https://doi.org/10.1016/j.radphyschem.2020.109026.
62. Aknouch, A., El-Ouardi, Y., Hamroud, L., Sebihi, R., Mouhib, M., Yjjou, M., Didi, A., & Choukri, A. (2021). A Monte Carlo study to investigate the feasibility to use the Moroccan panoramic irradiator in sterile insect technique programs. *Radiat. Environ. Biophys.*, *60*(4), 673–679. https://doi.org/10.1007/s00411-021-00934-6.
63. Saputro, B., Saputro, A. H., Nuraeni, N., Prasetio, H., Firmansyah, O. A., Fendinugroho, & Mayditia, H. (2024). Monte Carlo simulation as precision predictive tools to find isodose curve of gamma irradiator: A preliminary study. *Indones. J. Appl. Phys.*, *14*(2), 386. https://doi.org/10.13057/ijap.v14i2.93092.
64. Cao, V. C., Vo, A. T., Le, Q. T., Le, N. T., Duong, T. H., & Tran, H. N. (2021). Depth-dose profiles in continuous and discontinuous materials of food products and medical devices irradiated by 10 MeV electron beam. *J. Radioanal. Nucl. Chem.*, *330*(3), 609–617. https://doi.org/10.1007/s10967-021-07985-5.
65. Kroc, T. K. (2023). Monte Carlo simulations demonstrating physics of equivalency of gamma, electron-beam, and X-ray for radiation sterilization. *Radiat. Phys. Chem.*, *204*, 110702. https://doi.org/10.1016/j.radphyschem.2022.110702.
66. Jung, S. T., Pyo, S. H., Kang, W. G., Kim, Y. R., Kim, J. K., Kang, C. M., Nho, Y. C., & Park, J. S. (2021). Energy deposition calculation by Monte Carlo simulation in irradiation of electric cables by electron beam. *Radiat. Phys. Chem.*, *186*, 109506. https://doi.org/10.1016/j.radphyschem.2021.109506.
67. Kim, J., Moreira, R. G., & Castell-Perez, M. E. (2010). Simulation of pathogen inactivation in whole and fresh-cut cantaloupe (Cucumis melo) using electron beam treatment. *J. Food Eng.*, *97*(3), 425–433. https://doi.org/10.1016/j.jfoodeng.2009.10.038.
68. Kim, J., Rivadeneira, R. G., Castell-Perez, M. E., & Moreira, R. G. (2006). Development and validation of a methodology for dose calculation in electron beam irradiation of complex-shaped foods. *J. Food Eng.*, *74*(3), 359–369.
69. Hallman, G. J., & Loaharanu, P. (2016). Phytosanitary irradiation – Development and application. *Radiat. Phys. Chem.*, *129*, 39–45. https://doi.org/10.1016/j.radphyschem.2016.08.003.

70. Majer, M., Roguljić, M., Knežević, Ž., Starodumov, A., Ferenček, D., Brigljević, V., & Mihaljević, B. (2019). Dose mapping of the panoramic ^{60}Co gamma irradiation facility at the Ruđer Bošković Institute – Geant4 simulation and measurements. *Appl. Radiat. Isot.*, *154*, 108824. https://doi.org/10.1016/j.apradiso.2019.108824.
71. Kim, J., Moreira, R. G., & Castell-Perez, E. (2011). Optimizing irradiation treatment of shell eggs using simulation. *J. Food Sci.*, *76*(1), 173–177.
72. Kim, J., Kwon, S. -H., Chung, S. -W., Kwon, S. -G., Park, J. -M., & Choi, W. -S. (2013). Understanding phytosanitary irradiation treatment of pineapple using Monte Carlo simulation. *J. Biosyst. Eng.*, *38*(2), 87–94.
73. Kim, J., Moreira, R. G., & Castell-Perez, M. E. (2015). Improving phytosanitary irradiation treatment of mangoes using Monte Carlo simulation. *J. Food Eng.*, *149*, 137–143. https://doi.org/10.1016/j.jfoodeng.2014.10.005.
74. Kim, J., Moreira, R. G., & Castell-Perez, M. E. (2019). Determination of best pine wilt disease treatment using irradiation. *J. Radiat. Res. Appl. Sci.*, *12*(1), 269–280. https://doi.org/10.1080/16878507.2019.1650994.
75. Kim, J., Moreira, R. G., Rivadeneira, R., & Castell-Perez, M. E. (2005). Monte Carlo-based food irradiation simulator. *J. Food Process Eng.*, *29*(1), 72–88.
76. Kim, J., Moreira, R. G., Huang, Y., & Castell-Perez, M. E. (2007). 3-D dose distributions for optimum radiation treatment planning of complex foods. *J. Food Eng.*, *79*(1), 312–321.
77. Kim, J. (2014). Monte Carlo simulation of phytosanitary irradiation treatment for mangosteen using MRI-based geometry. *J. Biosyst. Eng.*, *39*(3), 205–214. https://doi.org/10.5307/JBE.2014.39.3.205(2014).
78. Peivaste, I., & Alahyarizadeh, G. (2019). Comparative study on absorbed dose distribution of potato and onion in X-ray and electron beam system by MCNPX2.6 code. *Mapan*, *34*(1), 19–29. https://doi.org/10.1007/s12647-018-0287-z.
79. Kataoka, N., Kawahara, D., & Sekiguchi, M. (2023). Uniform irradiation of table eggs in the shell with low-energy electron beams. *Radiat. Phys. Chem.*, *202*, 110553. https://doi.org/10.1016/j.radphyschem.2022.110553.
80. Sato, T., Iwamoto, Y., Hashimoto, S., Ogawa, T., Furuta, T., Abe, S. I., Kai, T., Matsuya, Y., Matsuda, N., Hirata, Y., Sekikawa, T., Yao, L., Tsai, P. E., Ratliff, H. N., Iwase, H., Sakaki, Y., Sugihara, K., Shigyo, N., Sihver, L., & Niita, K. (2024). Recent improvements of the particle and heavy ion transport code system – PHITS version 3.33. *J. Nucl. Sci. Technol.*, *61*(1), 127–135. https://doi.org/10.1080/00223131.2023.2275736.
81. Mannai, K., Askri, B., Loussaief, A., & Trabelsi, A. (2007). Evaluation using Geant4 of the transit dose in the Tunisian gamma irradiator for insect sterilization. *Appl. Radiat. Isot.*, *65*(6), 701–707.
82. El-Ouardi, Y., Aknouch, A., Dadouch, A., Mouhib, M., Maghnouj, A., Benmessaoud, M., & Yjjou, M. (2023). Control of transit doses by Monte Carlo simulation inside an ionization casemate housing of a ^{60}Co gamma irradiator. *Radiat. Phys. Chem.*, *206*, 110776. https://doi.org/10.1016/j.radphyschem.2023.110776.
83. Shiha, M., Cygler, J. E., MacRae, R., & Heath, E. (2023). 4D Monte Carlo dose reconstructions using surface motion measurements. *Phys. Med.*, *114*, 103135. https://doi.org/10.1016/j.ejmp.2023.103135.
84. Moon, S., Han, H., Choi, C., Shin, B., Son, G., Kim, H., Kim, S., Kim, J., Yoon, I. G., Lee, K. H., & Kim, C. H. (2024). Towards accurate dose assessment for emergency industrial radiography source retrieval operations: A preliminary study of 4D Monte Carlo dose calculations. *Nucl. Eng. Technol.*, *56*(12), 5428–5436. https://doi.org/10.1016/j.net.2024.09.004.
85. Gholampourkashi, S., Cygler, J. E., Lavigne, B., & Heath, E. (2020). Validation of 4D Monte Carlo dose calculations using a programmable deformable lung phantom. *Phys. Med.*, *76*, 16–27. https://doi.org/10.1016/j.ejmp.2020.05.019.
86. Loussaief, A., Trabelsi, A., & Baccari, B. (2006). Extended gamma sources modelling using multipole expansion: Application to the Tunisian gamma source load planning. *Radiat. Phys. Chem.*, *75*(4), 463–472.
87. Loussaief, A., & Trabelsi, A. (2007). Dose mapping using multipole moments. *Nucl. Instrum. Methods Phys. Res. Sect. A-Accel. Spectrom. Dect. Assoc. Equ.*, *580*(1), 102–105.
88. Rezaeian, P., Ataenia, V., & Shafiei, S. (2017). An analytical method based on multipole moment expansion to calculate the flux distribution in Gammacell-220. *Radiat. Phys. Chem.*, *141*, 339–345. https://doi.org/10.1016/j.radphyschem.2017.08.003.
89. Belkadhi, K., & Manai, K. (2016). Dose calculation using a numerical method based on Haar wavelets integration. *Nucl. Instrum. Methods Phys. Res. Sect. A-Accel. Spectrom. Dect. Assoc. Equ.*, *812*, 73–80. https://doi.org/10.1016/j.nima.2015.12.057.
90. Singh, M., & Datta, D. (2020). Development of an algorithm for gamma dose mapping in irradiated product using TOPSIS and its validation. *Radiat. Phys. Chem.*, *177*, 109123. https://doi.org/10.1016/j.radphyschem.2020.109123.
91. Studenikin, F. R., Bliznyuk, U. A., Chernyaev, A. P., Khankin, V. V., & Krusanov, G. A. (2021). Impact of aluminum plates on uniformity of depth dose distribution in object during electron processing. *Mosc. Univ. Phys. Bull.*, *76*(1), S1–S7. https://doi.org/10.3103/S0027134922010106.
92. Studenikin, F. R., Bliznyuk, U. A., Chernyaev, A. P., Krusanov, G. A., Nikitchenko, A. D., Zolotov, S. A., & Ipatova, V. S. (2023). Electron beam modification for improving dose uniformity in irradiated objects. *Eur. Phys. J. Spec. Top.*, *232*(10), 1631–1635. https://doi.org/10.1140/epjs/s11734-023-00886-6.
93. Bliznyuk, U. A., Borshchegovskaya, P. Y., Zolotov, S. A., Ipatova, V. S., Krusanov, G. A., Nikitchenko, A. D., Studenikin, F. R., & Chernyaev, A. P. (2022). Determining the electron beam spectrum after passing through aluminum plates. *Mosc. Univ. Phys. Bull.*, *77*(4), 615–621. https://doi.org/10.3103/S0027134922040038.
94. Bliznyuk, U. A., Avdyukhina, V. M., Borshchegovskaya, P. Y., Ipatova, V. S., Nikitchenko, A. D., Studenikin, F. R., & Chernyaev, A. P. (2021). Estimating the accuracy of reconstructing bichromatic spectra of electron beams from depth dose distributions. *Bull. Russ. Acad. Sci. Phys.*, *85*(10), 1108–1112. https://doi.org/10.3103/S1062873821100099.

95. Bliznyuk, U. A., Borshchegovskaya, P. Y., Ipatova, V. S., Nikitchenko, A. D., Studenikin, F. R., & Chernyaev, A. P. (2022). Determining the beam spectrum of industrial electron accelerator using depth dose distribution. *Bull. Russ. Acad. Sci. Phys.*, *86*(4), 500–507. https://doi.org/10.3103/S1062873822040062.
96. Sohrabpour, M., Hassanzadeh, M., Shahriari, M., & Sharifzadeh, M. (2002). Gamma irradiator dose mapping simulation using the MCNP code and benchmarking with dosimetry. *Appl. Radiat. Isot.*, *57*(4), 537–542. https://doi.org/10.1016/S0969-8043(02)00130-6.
97. Sohrabpour, M., Hassanzadeh, M., Shahriari, M., & Sharifzadeh, M. (2002). Dose distribution of the IR-136 irradiator using a Monte Carlo code and comparison with dosimetry. *Radiat. Phys. Chem.*, *63*, 769–772.
98. Raisali, G. R., & Sohrabpour, M. (1993). Application of EGS4 computer code for determination of gamma ray spectrum and dose rate distribution in Gammacell 220. *Radiat. Phys. Chem.*, *42*, 799–805.
99. Weiss, D. E., & Stangeland, R. J. (2003). Dose prediction and process optimization in a gamma sterilization facility using 3-D Monte Carlo code. *Radiat. Phys. Chem.*, *68*(6), 947–958.
100. Oliveira, C., Salgado, J., Botelho, M. L., & Ferreira, L. M. (2000). Dose determination by Monte Carlo – A useful tool in gamma radiation process. *Radiat. Phys. Chem.*, *57*(3/6), 667–670.
101. Oliveira, C., Salgado, J., & Ferro De Carvalho, A. (2000). Dose rate determinations in the Portuguese gamma irradiation facility: Monte Carlo simulations and measurements. *Radiat. Phys. Chem.*, *58*(3), 279–285.
102. Belchior, A., Botelho, M. L., & Vaz, P. (2007). Monte Carlo simulations and dosimetric studies of an irradiation facility. *Nucl. Instrum. Methods Phys. Res. Sect. A-Accel. Spectrom. Dect. Assoc. Equ.*, *580*(1), 70–72. https://doi.org/10.1016/j.nima.2007.05.040.
103. Portugal, L., Cardoso, J., & Oliveira, C. (2010). Monte Carlo validation of the irradiator parameters of the Portuguese gamma irradiation facility after its replenishment. *Appl. Radiat. Isot.*, *68*(1), 190–195.
104. Gharbi, F., Kadri, O., Farah, K., & Mannai, K. (2005). Validation of GEANT code of CERN as predictive tool of dose rate measurement in the Tunisian gamma irradiation facility. *Radiat. Phys. Chem.*, *74*(2), 102–110.
105. Kadri, O., Gharbi, F., & Farah, K. (2005). Monte Carlo improvement of dose uniformity in gamma irradiation processing using the GEANT4 code. *Nucl. Instrum. Methods Phys. Res. Sect. B-Beam Interact. Mater. Atoms*, *239*(4), 391–398.
106. Ounalli, L., Bhar, M., Mejri, A., Manai, K., Bouabidi, A., Abdallah, S. M., & Reguigui, N. (2017). Combining Monte Carlo simulations and dosimetry measurements for process control in the Tunisian Cobalt-60 irradiator after three half lives of the source. *Nucl. Sci. Tech.*, *28*(9), 1–10. https://doi.org/10.1007/s41365-017-0289-5.
107. Kim, Y. H., & Park, J. W. (2008). Dose rate simulation of a panoramic gamma irradiator using the MCNPX code and comparison with measurements. *J. Nucl. Sci. Technol.*, *45*, 325–328. https://doi.org/10.1080/00223131.2008.10875854.
108. Kang, C. M., Jung, S. T., Pyo, S. H., Seo, Y., Kang, W. G., Kim, J. K., Nho, Y. C., Park, J. S., & Choi, J. H. (2023). Characterization of the 2.5 MeV ELV electron accelerator electron source angular distribution using 3-D dose measurement and Monte Carlo simulations. *Nucl. Eng. Technol.*, *55*(12), 4678–4684. https://doi.org/10.1016/j.net.2023.09.004.
109. Khattab, K., Boush, M., & Alkassiri, H. (2013). Dose mapping simulation using the MCNP code for the Syrian gamma irradiation facility and benchmarking. *Ann. Nucl. Energy*, *58*, 110–112. https://doi.org/10.1016/j.anucene.2012.11.009.
110. Mortuza, M. F., Lepore, L., Khedkar, K., Thangam, S., Nahar, A., Jamil, H. M., Bandi, L., & Alam, Md K. (2018). Comissioning dosimetry and in situ dose mapping of a semi-industrial Cobalt-60 gamma-irradiation facility using Fricke and Ceric-cerous dosimetry system and comparison with Monte Carlo simulation data. *Radiat. Phys. Chem.*, *144*, 256–264. https://doi.org/10.1016/j.radphyschem.2017.08.022.
111. Gual, M. R., Milian, F. M., Mesquita, A. Z., & Pereira, C. (2017). New source models to represent the irradiation process in panoramic gamma irradiator. *Appl. Radiat. Isot.*, *128*, 175–182. https://doi.org/10.1016/j.apradiso.2017.06.046.
112. Gual, M. R., Mesquita, A. Z., Ribeiro, E., & Grossi, P. A. (2017). Shielding verifications for a gamma irradiation facility considering the installation of a new automatic product loading system. *Sci. Technol. Nucl. Install.*, *2017*, 1–6. https://doi.org/10.1155/2017/7408645.
113. Gual, M. R., Pereira, C., & Mesquita, A. Z. (2019). Application of a new source model of a panoramic gamma irradiator on dose map formation in an irradiated product. *Appl. Radiat. Isot.*, *144*, 87–92. https://doi.org/10.1016/j.apradiso.2018.12.002.
114. Aknouch, A., Elouardi, Y., Mouhib, M., Sebihi, R., Didi, A., & Choukri, A. (2020). New approach to make cylindrical packaging products in rotation around their fixed axis during irradiation in the Monte Carlo simulation. *Mosc. Univ. Phys. Bull.*, *75*(5), 447–450. https://doi.org/10.3103/S0027134920050045.
115. Aknouch, A., Mouhib, M., Sebihi, R., Didi, A., El-Ouardi, Y., Boubekraoui, A., & Choukri, A. (2020). Monte Carlo simulation of the dose rate distribution of a Moroccan panoramic gamma irradiator using the MCNPX code. *Mosc. Univ. Phys. Bull.*, *75*(1), 35–38. https://doi.org/10.3103/S0027134920010026.
116. Kataoka, N., Kawahara, D., & Sekiguchi, M. (2021). Surface treatment of eggshells with low-energy electron beam. *J. Radiat. Prot. Res.*, *46*(1), 8–13. https://doi.org/10.14407/JRPR.2020.